

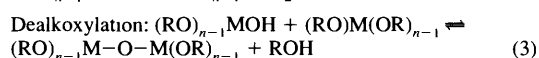
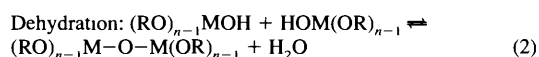
# Chemistry of Oxo-alkoxides of Metals

Ram C. Mehrotra and Anirudh Singh

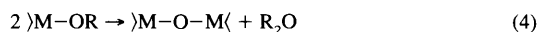
Department of Chemistry, University of Rajasthan, Jaipur-302 004, India

## 1 Introduction

In view of the extremely high ease of hydrolysis of metal alkoxides by even traces of moisture from any source (atmosphere, solvents, equipment, *etc.*), stringent precautions for maintenance of anhydrous environmental conditions have generally been regarded as essential for the synthesis of simple binary or heterometallic alkoxides in a pure state. However, from the 1950s, this facile hydrolytic susceptibility has been increasingly utilised in the sol-gel technique: the conversion of a metal alkoxide dissolved in an organic solvent (generally the parent alcohol) into a hydroxo-oxo-alkoxide 'sol,' followed by gelation and sintering to give the desired ceramic material. This development has led to much interest in the mechanism of the hydrolysis process and also in the actual composition of the hydroxo- or oxo-alkoxide derivatives formed. Early investigations by Bradley *et al.* have been summarised.<sup>1-3</sup> The simplest steps in the formation of metal oxo-alkoxide derivatives can be represented as follows by initial hydrolysis followed by dehydration and dealkoxylation reactions:



Evidence has been fast accumulating during the last decade or so that even in the absence of water, metal alkoxides may be converted into oxo-alkoxides by a number of possible mechanisms, *e.g.* elimination of ether:<sup>4</sup>

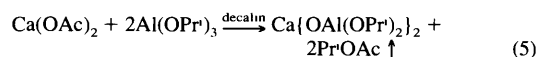


Doubts have also been raised recently about the reported formation of a trisisopropoxide by the straightforward reaction of metallic yttrium with isopropyl alcohol, as the derivative obtained was shown<sup>5a</sup> to correspond in analysis to  $\text{Y}_5\text{O(OPr)}_{13}$  the structure of

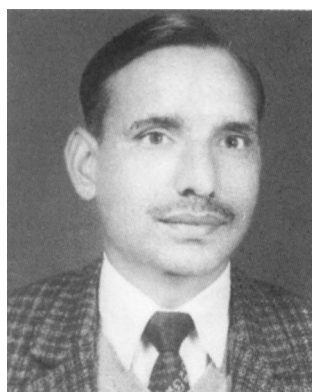
which was elucidated to correspond to  $[\text{Y}_5(\mu_5\text{-O})(\mu_3\text{-OPr})_4(\mu_2\text{-OPr})_4(\text{OPr})_5]$ , with the  $\mu_5\text{-O}$  atom at the base of a square pyramid of five yttrium atoms. Similar products have been isolated<sup>5b</sup> in similar reactions of metallic scandium, indium and ytterbium with isopropyl alcohol. The reaction of neodymium metal with isopropyl alcohol yielded<sup>5c</sup> the solvated pentanuclear  $[\text{Nd}_5(\mu_5\text{-O})(\mu_3\text{-OPr})_2(\mu_2\text{-OPr})_6(\text{OPr})_5(\text{Pr}^i\text{OH})_2]$ , in which the  $\mu_5\text{-O}$  atom is surrounded by a trigonal-bipyramid of neodymium atoms. In the first paper<sup>5a</sup> of this series, the authors had carefully checked that 'the obtention of previously reported  $[\text{Y}\{\text{Al(OPr)}_4\}_3]$  in high yield (up to 70%) with respect to the amount of metal consumed suggests that non-oxo species are predominant in the initial reaction solution', and that the formation of the oxo-species, which does not react with  $\text{Al(OPr)}_3$  to form the heterometallic derivative  $[\text{Y}\{\text{Al(OPr)}_4\}_3]$ , 'results mainly from the structural modifications induced by the removal of  $\text{Pr}^i\text{OH}$  ligands in order to achieve the most favoured coordination number of six for yttrium atoms in alkoxide derivatives.' Similar comments have been made<sup>5d</sup> later on such findings by Mehrotra.

Isolation of similar types of oxo-species for barium,  $[\text{HBa}_5\text{O(OPh)}_9(\text{thf})_8(\text{thf} = \text{tetrahydrofuran}), [\text{H}_3\text{Ba}_6\text{O}(\text{OBu}^i)_{11}(\text{OCEt}_2\text{CH}_2\text{O})(\text{thf})_3]$ <sup>6a</sup> and  $[\text{H}_4\text{Ba}_6(\mu_6\text{-O})(\mu_3\text{-}\eta^2\text{-OC}_2\text{H}_4\text{OMe})_8(\eta^2\text{-OC}_2\text{H}_4\text{OMe})_4(\text{OC}_2\text{H}_4\text{OMe})_2]$ <sup>6b</sup> as well as for calcium,  $[\text{Ca}_6(\mu_4\text{-O})_2(\mu_3\text{-OEt})_4(\text{OEt})_4] \cdot 14\text{EtOH}$ <sup>7</sup> by the reactions of these metals with the appropriate phenol or alcohol illustrates the diversity of oxo-products obtained in straightforward reactions expected to yield the simple binary alkoxides; the formation of a derivative,  $[\text{H}_3\text{Ba}_6\text{O}(\text{OBu}^i)_{11}(\text{OCEt}_2\text{CH}_2\text{O})(\text{thf})_3]$  with a diolate component,  $(\text{OCEt}_2\text{CH}_2\text{O})$  has been explained<sup>6a</sup> as arising from a side reaction involving the solvent, tetrahydrofuran, used in the reaction rather than from the reacting alcohol.

Besides the above rather sporadic products, a number of bimetallic  $\mu$ -oxo-alkoxides with the general formula,  $(\text{RO})_{n-1}\text{-M}'\text{-O-M}''\text{-O-M}'\text{-(OR)}_{n-1}$ , where  $\text{M}' = \text{Al}^{\text{III}}$  ( $n = 3$ ) or  $\text{Ti}^{\text{IV}}$  ( $n = 4$ ) and  $\text{M}'' = \text{Cr}^{\text{II}}, \text{Mn}^{\text{II}}, \text{Fe}^{\text{II}}, \text{Co}^{\text{II}}, \text{Ni}^{\text{II}}, \text{Zn}^{\text{II}}, \text{Mo}^{\text{II}}, \text{Ca}^{\text{II}}$  or  $\text{R}_2\text{Sn}^{\text{II}}$ <sup>8,9</sup> have been systematically synthesized<sup>9</sup> by reactions of the type:



Anirudh Singh is Associate Professor of Chemistry at the University of Rajasthan, Jaipur, from where he obtained his PhD under Professor R. C. Mehrotra. He spent three years (1979-82) as a SERC Postdoctoral Fellow with Professor M. F. Lappert at the University of Sussex, followed by three months in 1987 as a Visiting Scientist. Dr. Singh is an inorganic and organometallic chemist with



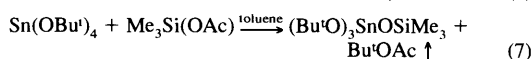
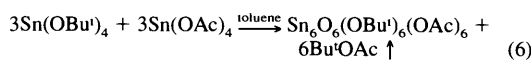
particular current interests in molecular design and characterization of homo- and hetero-metallo-organic precursors for better ceramic and catalytic materials. He is the author/coauthor of over 100 research papers, review articles, and course-work for Open Universities in areas of his speciality. With Professor R. C. Mehrotra, he coauthored the widely appreciated book 'Organometallic Chemistry: A Unified Approach'.

With more than four decades of research experience on M-O-C derivatives, synthesis and characterization of a large variety of

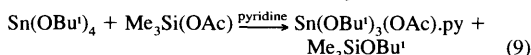
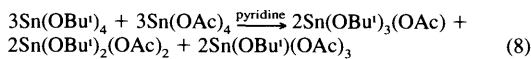


heterometallic alkoxides has been the unique contribution from the research school of Professor Emeritus R. C. Mehrotra [MSc, DPhil (Ald.), PhD, DSc (London)] during the past two decades. Author/coauthor of more than 600 research papers, dozens of review articles, and chapters in well-known treatises. Mehrotra has supervised the research work of more than 100 scholars, who have themselves won covetable honours in their own careers.

In recent publications<sup>10</sup> describing the reactions between  $\text{Sn}(\text{OBu}^t)_4$  and  $\text{Sn}(\text{OAc})_4$  as well as with  $\text{Me}_3\text{Si}(\text{OAc})$  in a refluxing hydrocarbon (toluene) solvent, the ester *tert*-butyl acetate was eliminated resulting in Sn–O–Sn and Sn–O–Si derivatives:

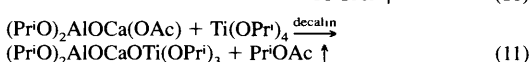
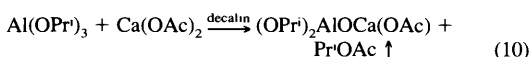


However, only ligand exchanges of the following types were found to occur when the reactions were carried out in a coordinating solvent, pyridine:

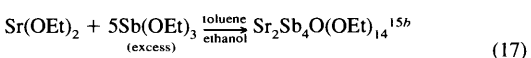
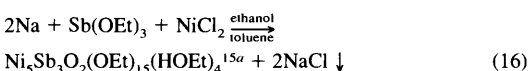
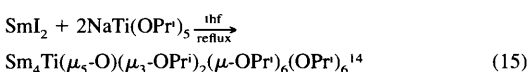
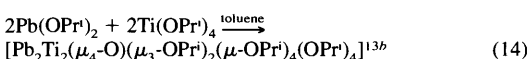
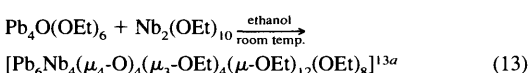
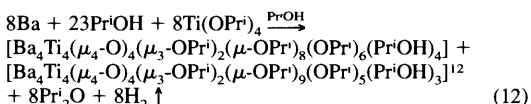


The bimetallic  $\mu$ -alkoxides are generally soluble in organic solvents and are, therefore, attractive precursors for the sol–gel process.

Ester elimination reactions using different metal alkoxides in stepwise reactions can lead<sup>11</sup> to tri- or even higher heterometallic  $\mu$ -oxo-alkoxides, e.g.:



Besides the above ester elimination method, heterometallic oxo-alkoxides have been synthesized by a variety of procedures, some of which are illustrated by the following typical examples:



Although there has been a slight lingering scepticism that the formation of such homo- as well as hetero-metallic oxo-alkoxide species might be due to some side hydrolysis of the normal alkoxy products, the rapidly increasing number of reports of investigations carried out under stringently anhydrous conditions have led to conclusions (cf. Section 4) about the formation of these oxo-products by side reactions involving the elimination of ether<sup>4</sup> or alkene–ketone<sup>16</sup> molecules.

However, in spite of the rapidly increasing number of reports about the isolation of oxo-alkoxides of various metals and their definitive characterization by X-ray crystal structure determination, much work in this area is somewhat unplanned and sporadic. The products have in general been isolated in rather low yields with insufficient effort to identify the other reactions that occur simultaneously. Further, except in a few cases, efforts at correlation of results, even by those who have reported a number of distinct oxo-alkoxide derivatives, are not exhaustive.

The main aim of this review on homo- and hetero-metal oxo-alkoxides (although a few related products, e.g., acetato–acetylacetonato species have also been included for comparison) is to summarize the salient features of the current (up to early 1995) knowledge about the isolation and significant structural features of metal oxo-alkoxides in the hope that it would lead to more penetrating and quantitative studies on a larger number of systems with plausible and correlated explanations for their formation and structural features, which should encourage more intensive and focused further investigations.

## 2 Homometallic Oxo-alkoxides

### 2.1 Preparation

These can be prepared in a few typical cases by the direct controlled hydrolysis of simple binary metal alkoxides. However, most of these have been obtained inadvertently during efforts to prepare the normal alkoxides, and a few of these types are grouped together under the heading ‘sporadic formation’ in Section 2.1.3.

#### 2.1.1 Direct Hydrolytic Reaction

Hydroxy-alkoxides obtained initially in the hydrolysis of metal alkoxides (equation 1) are easily converted into oxo-alkoxides by dehydration and dealkylation reactions (equations 2 and 3). Formation of mixtures of such hydroxy- and oxo-alkoxides during the hydrolysis of metal alkoxides in any molar ratio and their identification has assumed special significance in the sol–gel process<sup>1–3</sup> of preparing ceramic materials from metal alkoxides (cf. Section 4).

The formation of a number of oxo-alkoxides of titanium was described by Bradley *et al.*<sup>1</sup> during their extensive studies on the variations in the molecular complexities of metal oxo-alkoxide species by the changes observed in molecular mass (measured by ebulliometry) on slow addition of water to a solution of the alkoxide in the alcohol. Watenpaugh and Caughlan,<sup>17a</sup> however, elucidated the crystal structure of  $\text{Ti}_7\text{O}_4(\text{OEt})_{20}$  (Figure 1), which was confirmed in 1991 by Schmid *et al.*<sup>17b</sup> who also elucidated the structures of two other titanium oxo-alkoxide polymorphs with the composition  $[\text{Ti}_{16}\text{O}_{16}(\text{OEt})_{32}]$  formed during further hydrolysis of  $\text{Ti}(\text{OEt})_4$ . The structure (Figure 2) of  $[\text{Nb}_8\text{O}_{10}(\text{OEt})_{20}]^{17c}$  was elucidated in 1968, followed by that of  $[\text{Zr}_{13}\text{O}_8(\text{OMe})_{36}]^{17d}$  (Figure 3) in 1977 and of  $[\text{Sn}_6\text{O}_4(\text{OMe})_4]^{17e}$  (Figure 4) in 1978; these oxo-alkoxides were all isolated by controlled hydrolysis of the corresponding metal alkoxides. A partially hydrolysed crystalline species,  $(\text{LiOBu}^t)_{10}(\text{LiOH})_6$  has recently been isolated<sup>18</sup> by prolonged exposure of a concentrated solution of  $\text{LiOBu}^t$  in hexane to moist air.

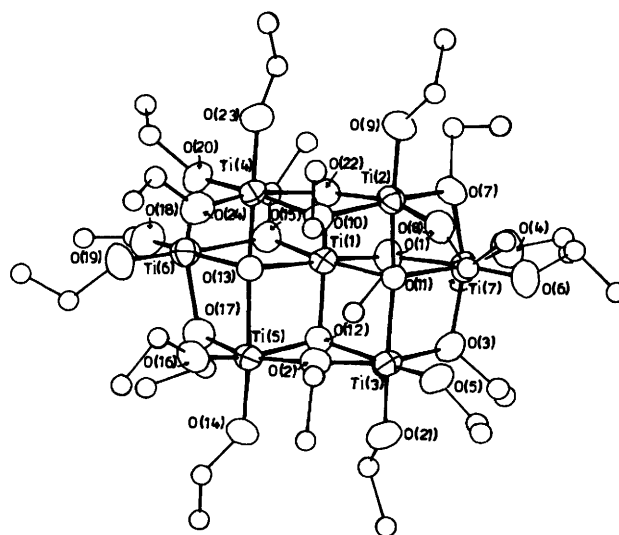
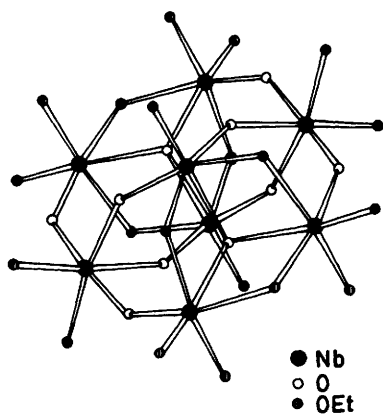
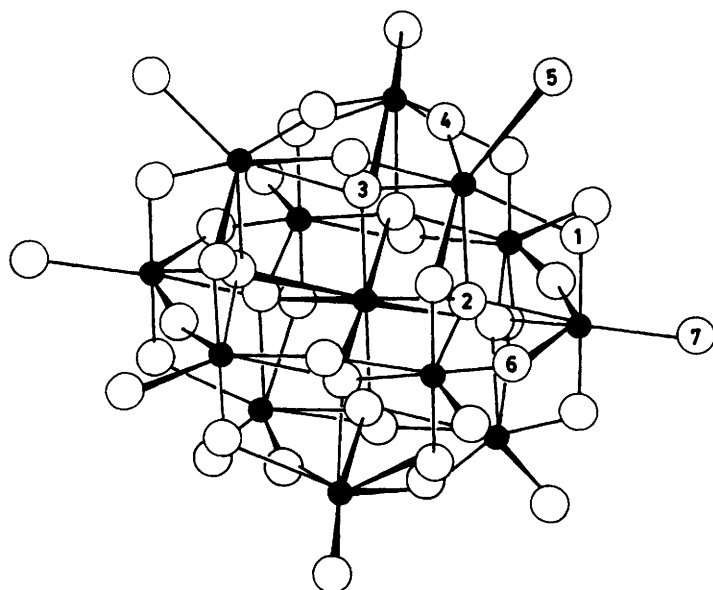
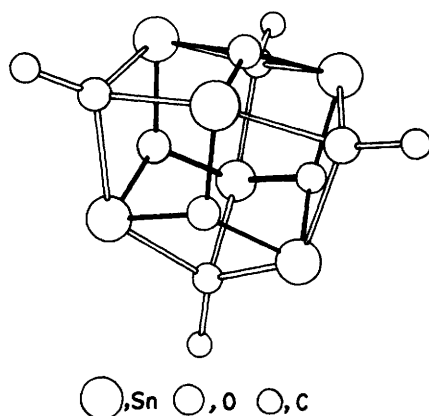
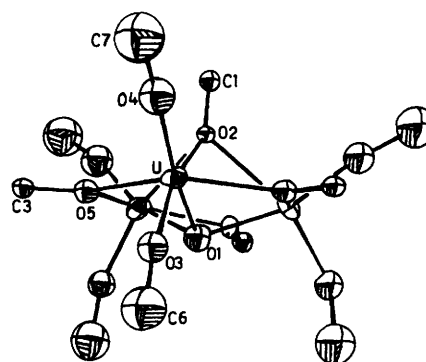


Figure 1 The X-ray structure of  $\text{Ti}_7\text{O}_4(\text{OEt})_{20}$ .<sup>17a,b</sup>


 Figure 2 The X-ray structure of  $\text{Nb}_8\text{O}_{10}(\text{OEt})_{20}$ .<sup>17c</sup>

 Figure 3 The X-ray structure of  $\text{Zr}_{13}\text{O}_8(\text{OMe})_{36}$ .<sup>17d</sup>

 Figure 4 The X-ray crystal structure of  $\text{Sn}_6\text{O}_4(\text{OMe})_4$ .<sup>17e</sup>

### 2.1.2 Reactions of Metal Oxo-chlorides with Alkali Alkoxides

As in the preparation of simple binary alkoxides by the reactions of metal halides with alkanols in the presence of a proton acceptor base, the monomeric  $\text{UO}_2(\text{OBu}^t)_2(\text{Ph}_3\text{PO})_2$ <sup>19a</sup> and  $\text{VO}(\text{OCH}_2\text{CH}_2\text{Cl})_3$ <sup>19b</sup> as well as other vanadium oxo-alkoxides with bulky and chiral alcohols<sup>19c</sup> have been synthesized from the reactions of  $\text{UO}_2\text{Cl}_2$  and  $\text{VOCl}_3$  with the corresponding alkali alkoxides.

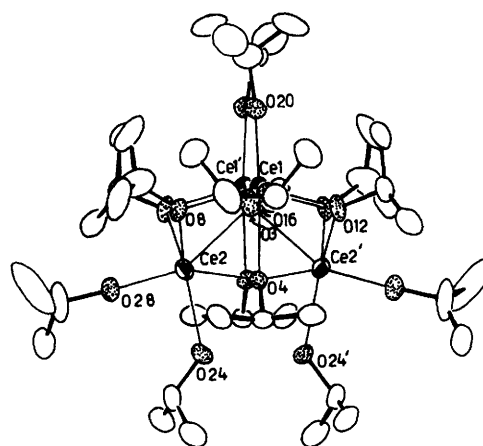
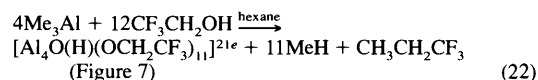
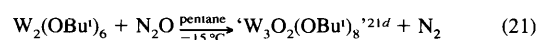
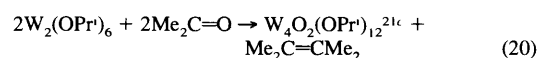
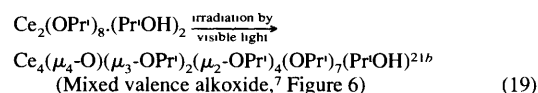
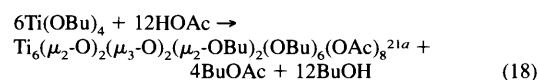

 Figure 5 The X-ray structure of  $\text{U}_3\text{O}(\text{OBu}^t)_{10}$ .<sup>20</sup>

In contrast to the above straightforward reactions yielding the expected oxo-alkoxides, an unusual trinuclear oxo-alkoxide of uranium,  $\text{U}_3\text{O}(\text{OBu}^t)_{10}$ ,<sup>20</sup> (Figure 5) was obtained in the reaction between  $\text{UCl}_4$  and  $\text{K}(\text{OBu}^t)$ .

### 2.1.3 Formation of Oxo-alkoxides in Other Non-hydrolytic Procedures

In addition to the isolation of the unexpected trinuclear product in the reaction of uranium tetrachloride with potassium *tert*-butoxide, multinuclear oxo-alkoxides of a number of electropositive metals, *e.g.*, yttrium,<sup>5a</sup> scandium, indium, ytterbium,<sup>5b</sup> and neodymium<sup>5c</sup> as well as those of barium<sup>6</sup> and calcium<sup>7</sup> have been isolated in the reactions of these metals with alcohols, which were normally expected to yield the simple binary alkoxides. Although the mechanism of the formation of such oxo-alkoxides is not yet fully understood, the initial scepticism about their formation under stringently anhydrous conditions has gradually been dispelled.

Besides the above, the isolation of a few other oxo-alkoxides by rather novel routes can be represented by the following equations:


 Figure 6 The X-ray structure of  $\text{Ce}_4\text{O}(\text{OPr})_{13}(\text{Pr}^t\text{OH})^{21b}$

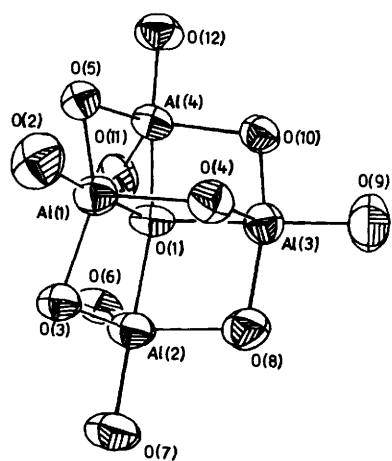


Figure 7 The X-ray structure of  $[Al_4O(OCH_2CF_3)_{11}]^{2+}$

## 2.2 Spectroscopic Properties

Of the different spectroscopic (IR, NMR, mass and XANES) techniques, the contribution of IR studies<sup>5a-c,7,19a-b,21a,22</sup> is generally limited to indicating the presence of  $\nu(M-O)$ ,  $\nu(M=O)$ ,  $\nu(C-O)M$  and  $\nu(RO)M$  (terminal/bridging).

By contrast,  $^1H$  and  $^{13}C$  NMR studies<sup>5a-c,10,19a-b,21b,22</sup> provide in many instances useful information regarding the environments of the alkoxy groups and their ligation (terminal,  $\mu_2$ -,  $\mu_3$ -bridging): e.g. the room temperature  $^1H$  NMR spectra of  $M_5(\mu_5-O)(\mu_3-OPr^i)_4(\mu_2-OPr^i)_4(OPr^i)_5$  ( $M = Sc, Y^{5a}$ ) (in  $C_6D_6$  at 250 MHz) show four sharp doublets and associated septets in the ratio 4:4:4:1, consistent with the requirements of the single crystal X-ray structures shown in Figure 8. Other examples exhibiting similar structural features both in solution and in the solid state include, *inter alia*,  $Y_5O(OPr^i)_{13}$ ,<sup>5a</sup>  $Ce_4O(OPr^i)_{13}(Pr^iOH)$ ,<sup>21b</sup>  $Mo_3O(OPr^i)_{10}$ .<sup>22</sup>

However, owing to insufficient resolution even at lower temperatures, NMR spectroscopy remains of limited utility even as corroborative evidence of the structures in the solid state. For example, the  $^1H$  NMR spectrum of  $In_5(\mu_5-O)(\mu_3-OPr^i)_4(\mu_2-OPr^i)_4(OPr^i)_5$ <sup>5b</sup> at room temperature shows only two types of isopropoxo group environments in the ratio 8:5, and  $^1H$  NMR peaks observed even at  $-80^\circ C$  are not in good agreement with the solid state structure (Figure 8). With the availability of definite single crystal X-ray structures of an increasing number of oxo-alkoxides (see Figures 1–8 and Table 1), information from NMR spectroscopy for sufficiently rigid molecules assumes special significance in cases for which X-ray data are not yet available.

One advantage of the NMR technique is that information is available about molecular dynamics (e.g. fluxionality). For example, such behaviour is reflected in the variable-temperature  $^1H$  NMR spectra of  $In_5O(OPr^i)_{13}$ ,<sup>5b</sup> which demonstrate: (i) the greater lability of isopropoxo groups in the indium derivative, (ii) the rapid exchange of  $\mu_2$ - and  $\mu_3$ -alkoxy groups above  $-30^\circ C$  ( $\Delta G$  43–49

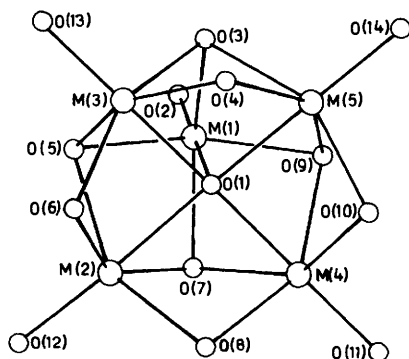


Figure 8 The X-ray structure of  $M_5O(OPr)_{13}$  ( $M = Y^{5a}, In, Yb^{5b}$ ) (only the metal–oxygen core is represented).

$\text{kJ mol}^{-1}$ ), and (iii) the inseparable resonance of the terminal isopropoxo groups at  $-80^\circ C$ . These observations tend to suggest that either the terminal basal–apical exchange is more rapid than  $\mu_2$ – $\mu_3$ -bridging exchange or, more likely, the chemical shifts of the basal and apical terminal ligands are too close for resolution.

$^{29}Si$  and  $^{17}O$  NMR spectroscopy has been utilized in recent years to elucidate the mechanism of hydrolysis of silicon and titanium alkoxides (see Section 4).  $^{17}O$  NMR chemical shifts provide information on the number of metal atoms linked to an oxo-ligand (i.e. connectivity) as illustrated by the variation in the chemical shifts of oxo ligands in the order  $OTi_2 > OTi_3 > OTi_4$ , which are observed in the ranges  $\delta$  650–850, 450–650 and 250–450, respectively.  $^{29}Si$  NMR spectra indicate environments of silicon atoms, e.g., the number of oxygens to which a central silicon atom is directly bonded.

The importance of metal ( $^{89}Y$ ,  $^{119}Sn$ ,  $^{207}Pb$ , etc.) NMR spectral studies of oxo-alkoxides has recently been exhibited for ascertaining the purity of a compound and for indicating the coordination number of the metal atoms and their geometry. For example, the  $^{89}Y$  NMR spectrum of  $Y_5(\mu_5-O)(\mu_3-OPr^i)_4(\mu_2-OPr^i)_4(OPr^i)_5$ <sup>5a</sup> shows resonances at  $\delta$  –13.2 and –16.9 in a 1:4 intensity ratio, consistent with the X-ray structure (Figure 8). In view of the inherent difficulties<sup>1b</sup> in X-ray structure determinations of metal alkoxides in general, it may be that the applications of more sophisticated NMR techniques should soon prove to be an adequate substitute for X-ray crystallography.

Although only a few XANES studies, of titanium oxo-alkoxide derivatives, are at present available, the potential of this technique is promising for structural elucidation.

Mass spectral studies<sup>5b</sup> of  $M_5O(OPr^i)_{13}$  ( $M = Sc, Y, Yb$ ) have established that the pentanuclear species is maintained in the gas phase. For scandium, the  $Sc_5O(OPr^i)_{12}^+$  ion was the most abundant metal-containing species, whereas  $Yb_5O(OPr^i)_{10}^+$  gave the highest mass peak for the ytterbium derivative. Interestingly the indium analogue was too thermally unstable to give a mass spectrum.

## 2.3 Structural Features

The structures of metal oxo-alkoxides of only a few metals, such as  $Ti$ ,<sup>17a,b</sup>  $Zr$ ,<sup>17d</sup>  $Nb$ <sup>17c</sup> and  $Sn$ <sup>17e</sup> had been determined up to 1980. Since then crystal structures of a large number (Table 1) of metal oxo-alkoxides have been elucidated, revealing several novel features, as illustrated (see Figures 1–8) by a few typical examples. Concurrently, advances in the understanding of the nature of these species in solution have been made through the use of multinuclear NMR techniques.

The oxo-ligand can bond to metal clusters and cages in several modes (Figure 9). The oxo-group formally considered as  $O^{2-}$  is an extremely versatile ligand. As a terminal ligand, the oxo-group in principle can bind as a linear six-electron ( $M\equiv O$ ) or four-electron ( $M=O$ ) ligand, the later being more common in mononuclear metal oxo-alkoxides. As a bridging group, there are several possibilities:  $\mu_3^-$ ,  $\mu_4^-$ ,  $\mu_5^-$  and  $\mu_6^-$ , changes from one form to another may result from environmental requirements. These possible bonding types are illustrated in Figure 9, along with a few examples of those (including some hetero-metal species) which have been so far characterized by X-ray crystallography. These interesting varieties of derivatives can be classified in a number of ways according to: (a) the mode of bonding of the oxo-ligand to the metals; (b) the nuclearity of the species (Table 1); and (c) the metal atom–oxygen core. For convenience we present a brief account of the structural features of the metal oxo-alkoxides according to the nuclearity of the derivatives, which appears to be influenced mainly by factors like the steric demand of the alkoxy groups, the size of the metal atoms, and the preferred geometry of the metal atoms.

## 2.4 Reactivity

Although the chemical reactivity of metal oxo-alkoxides has not received much attention, the results that have emerged so far indicate interesting possibilities.

**Table 1** Summary of the structural features of a few typical homometallic oxo-alkoxides<sup>a</sup>

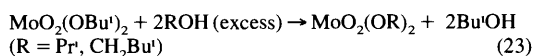
| Compound<br>(Metal oxygen core)  | Geometry of the<br>oxo ligand and<br>(Bridging mode) | Coordination<br>number<br>(Geometry)*<br>of the metal | Space<br>group                             | Z      | Comments  |
|--|--|---|--|--------|---|
| <b>Mononuclear derivatives</b>   |  |   |  |        |   |
| VO(OCH <sub>2</sub> CH <sub>2</sub> Cl <sub>3</sub> ) <sup>19b</sup><br>(VO <sub>4</sub> )   | Terminally bonded                                    | 4<br>(Trigonal pyramid)                               | $P\bar{1}$                                 | 2      | The molecule consists of a flat trigonal pyramidal array of oxygens around vanadium in a monomeric unit, dimerization of molecules <i>via</i> long V–OR bonds [2 261(2) Å], leads to a trigonal bipyramidal geometry for each monomeric unit  |
| UO <sub>2</sub> (OBU <sup>t</sup> ) <sub>2</sub> (Ph <sub>3</sub> PO) <sub>2</sub> <sup>19a</sup><br>(UO <sub>6</sub> )  | Terminally bonded                                    | 6<br>(Pseudo Oh)                                      | $P2_1/n$                                   | 4      | The structure consists of monomeric units in which the uranium atom is in a pseudooctahedral environment of oxygen atoms, and the oxo groups lie <i>trans</i> to one another, the <i>cis</i> -arrangement of four monodentate ligands in the equatorial plane has no precedent in the structural chemistry of uranyl compounds  |
| <b>Polynuclear derivatives</b><br>(Arranged in order of increasing nuclearity)   |  |   |  |        |   |
| Mo <sub>3</sub> (μ <sub>3</sub> -O)(μ <sub>3</sub> -OPr <sup>t</sup> )(μ <sub>2</sub> -OPr <sup>t</sup> ) <sub>3</sub><br>(OPr <sup>t</sup> ) <sub>6</sub> <sup>22</sup><br>(Mo <sub>3</sub> O <sub>11</sub> )   | Trigonal pyramid<br>(μ <sub>3</sub> )                | 6<br>(Oh)   | $P\bar{1}$                                 | 4      | Mo–O(μ <sub>3</sub> -OPr <sup>t</sup> ) = 2 19(3) Å(av), Mo–O(μ <sub>3</sub> -oxo) = 2 04(3) Å(av), Mo–O(μ <sub>2</sub> -OPr <sup>t</sup> ) = 2 03(3) Å(av), Mo–O (terminal OPr <sup>t</sup> ) = 1 88(3) Å and 1 95(3) Å when they are <i>trans</i> to the capping alkoxide and oxo ligand respectively, <i>trans</i> -influence oxo > OPr <sup>t</sup> , Mo–Mo = 2 53 Å(av)  |
| W <sub>3</sub> (μ <sub>2</sub> -O) <sub>2</sub> (OBU <sup>t</sup> ) <sub>8</sub> <sup>21d</sup><br>(W <sub>3</sub> O <sub>10</sub> )   | Bent<br>(μ <sub>2</sub> )                            | 5/4/3<br>with respect to W–O<br>bonding               | $P2_1/n$                                   | 4      | The structure is without precedent no capping μ <sub>3</sub> ligand, two types of W–W bonds two long (2 93 Å) and one short (2 45 Å), each tungsten atom is in a unique coordination environment, both the oxo ligands are in the W <sub>3</sub> plane and bridge the two long W–W distances  |
| U <sub>3</sub> (μ <sub>3</sub> -O)(μ <sub>3</sub> -OBU <sup>t</sup> )(μ <sub>2</sub> -OBU <sup>t</sup> ) <sub>3</sub><br>(OBU <sup>t</sup> ) <sub>6</sub> <sup>20</sup><br>(U <sub>3</sub> O <sub>11</sub> )   | Trigonal pyramid<br>(μ <sub>3</sub> )                | 6<br>(Distorted Oh)                                   | $P6_3/mc$                                  | 2      | The trinuclear unit (Figure 5) consists of three distorted mutually confacial octahedra sharing an edge with C <sub>3v</sub> crystallographic symmetry, U–U = 3 574(1) Å, indicating their non-bonded nature  |
| [Al <sub>4</sub> (μ <sub>4</sub> -O)(μ <sub>2</sub> -OCH <sub>2</sub> CF <sub>3</sub> ) <sub>5</sub><br>(OCH <sub>2</sub> CF <sub>3</sub> ) <sub>6</sub> ] <sup>–21e</sup><br>(Al <sub>4</sub> O <sub>12</sub> )   | Highly distorted Td<br>(μ <sub>4</sub> )             | 5<br>(Distorted TBP)                                  | $Pna2_1$                                   | 4      | All aluminium atoms are five-coordinate (Figure 7), the molecular anion contains two-, three- and four-coordinate oxygen atoms  |
| Ce <sub>4</sub> (μ <sub>4</sub> -O)(μ <sub>3</sub> -OPr <sup>t</sup> ) <sub>2</sub> (μ <sub>2</sub> -OPr <sup>t</sup> ) <sub>4</sub><br>(OPr <sup>t</sup> ) <sub>7</sub> (PrOH) <sub>2</sub> <sup>21b</sup><br>(Ce <sub>4</sub> O <sub>15</sub> )  | Butterfly form<br>(μ <sub>4</sub> )                  | 6/7   | $C2/c$                                     | 4      | The molecule (Figure 6) possesses a crystallographic C <sub>2</sub> axis that passes through the oxo ligand and the centre of a symmetric hydrogen bond between the coordinated alcohol and one terminal alkoxide   |
| M <sub>5</sub> (μ <sub>5</sub> -O)(μ <sub>3</sub> -OPr <sup>t</sup> ) <sub>4</sub> (μ <sub>2</sub> -OPr <sup>t</sup> ) <sub>4</sub><br>(OPr <sup>t</sup> ) <sub>5</sub> <sup>5a,b</sup><br>[M = Sc, Y, <sup>5a</sup> In, <sup>5b</sup> Yb <sup>5b</sup> ]<br>(M <sub>5</sub> O <sub>14</sub> ) | SPyr<br>(μ <sub>5</sub> )                            | 6<br>(Distorted Oh)                                   | $Pbca$ (M = Y)<br>$P2_1/n$<br>(M = In, Yb) | 8<br>4 | All the three derivatives are isostructural (Figure 8), M–O distances follow the pattern μ <sub>3</sub> -OR ≈ μ <sub>5</sub> -O (oxo) > μ <sub>2</sub> -OR > terminal OR (R = Pr <sup>t</sup> ), angles M–O–C to terminal ligands are nearly linear   |
| Nd <sub>5</sub> (μ <sub>5</sub> -O)(μ <sub>3</sub> -OPr <sup>t</sup> ) <sub>2</sub> (μ <sub>2</sub> -OPr <sup>t</sup> ) <sub>6</sub><br>(OPr <sup>t</sup> ) <sub>5</sub> (PrOH) <sub>2</sub> <sup>5c</sup><br>(Nd <sub>5</sub> O <sub>16</sub> )   | TBP<br>(μ <sub>3</sub> )                             | 6<br>(Distorted Oh)                                   | $Aba2$                                     | 4      | The Nd–O distances vary from 2 121(9) to 2 719(1) Å, with the longest Nd–O distance involving the μ <sub>5</sub> -O ligand, the Nd–O distances vary in the order μ <sub>5</sub> -O ≈ Nd–O(H)Pr <sup>t</sup> > μ <sub>3</sub> -OPr <sup>t</sup> > μ <sub>2</sub> -OPr <sup>t</sup> > terminal OPr <sup>t</sup> , the μ <sub>5</sub> -oxo ligand in a trigonal bipyramidal environment is unprecedented for an oxo-alkoxide |

Table 1 contd

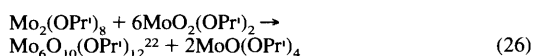
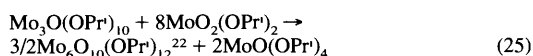
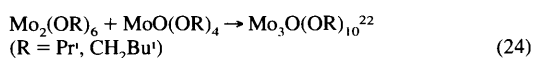
| Compound<br>(Metal oxygen core)   | Geometry of the<br>oxo ligand and<br>(Bridging mode) | Coordination<br>number<br>(Geometry)*<br>of the metal                                | Space<br>group | Z | Comments   |
|---|--|--|----------------|---|--|
| $\text{H}_3\text{Ba}_6(\mu_5\text{-O})(\mu_3\text{-OBU}^t)_5$<br>( $\mu_2\text{-OBU}^t)_3(\text{OBU}^t)$<br>( $\text{OCeEt}_2\text{CH}_2\text{O})(\text{thf})_3^{6a}$<br>( $\text{Ba}_6\text{O}_{16}$ ) | SPyr<br>( $\mu_5$ )                                  | 6/5<br>(Distorted Oh/TBP)  | $P1$           | 2 | Barium atoms associated with the $\text{Ba}_5(\mu_5\text{-O})$ pyramid are six-coordinate, while the sixth barium atom is only five-coordinate, five coordination for barium is unprecedented  |
| $\text{Ca}_6(\mu_4\text{-O})_2(\mu_3\text{-OEt})_4(\text{OEt})_4$<br>( $\text{EtOH}$ ) $_{14}^7$<br>( $\text{Ca}_6\text{O}_{24}$ )  | Distorted Td<br>( $\mu_4$ )                          | 6<br>(Distorted Oh)  | $P2_1/c$       | 2 | In the hexanuclear complex the metal-oxygen framework is built of two $\text{Ca}_4\text{O}_2$ cubes sharing a common $\text{Ca}_4\text{O}_2$ face, which involves both $\mu_4$ -oxo ligands O(1) and O(1a), the other oxygen vertices of the cubes are occupied by the $\mu_3$ -OEt groups. The central [Ca(1) and Ca(1a)] and the other four peripheral calcium atoms are associated with two and three $\mu_3$ -OEt groups, respectively |
| $\text{Sn}_6(\mu_3\text{-O})_4(\mu_3\text{-OMe})_4^{17c}$<br>( $\text{Sn}_6\text{O}_8$ )  | Triangular<br>( $\mu_3$ )                            | 5, lone pair of<br>electrons occupying<br>the equatorial<br>position<br>(Pseudo TBP) | $P2_1/c$       | 4 | The $\text{Sn}_6\text{O}_4(\text{OME})_4$ units with a central $\text{Sn}_6\text{O}_4$ core possessing the adamantane structure (Figure 4), the Sn-O distances [2.05(1)—2.08(1) Å] are amongst the shortest than those typically recorded for bivalent tin-oxygen compounds  |
| $\text{Ti}_6(\mu_2\text{-O})_2(\mu_3\text{-O})_2(\mu_2\text{-OBU})_2$<br>( $\text{OBU}$ ) $_6(\text{OAc})_8^{21a}$<br>( $\text{Ti}_6\text{O}_{28}$ )  | Bent/trigonal planar<br>( $\mu_4/\mu_3$ )            | 6<br>(Oh)  | $P2_1/c$       | 2 | The structure consists of two $\text{Ti}_2\text{O}_{10}$ (two edge-sharing octahedra) units linked by two corner sharing octahedra, the titanium atoms are in nonequivalent environments, Ti-O distances vary from 1.742 to 2.742 to 2.148 Å (average 1.962 Å)   |
| $\text{Ti}_7(\mu_4\text{-O})_2(\mu_3\text{-O})_2(\mu_3\text{-OEt})_8$<br>( $\text{OEt}$ ) $_{12}^{17ab}$<br>( $\text{Ti}_7\text{O}_{24}$ )  | Td/trigonal planar<br>( $\mu_4/\mu_3$ )              | 6<br>(Highly distorted Oh)   | $P1$           | 2 | The seven titanium atoms are linked by three different types of oxygen bridges (Figure 1) two $\mu_4$ -O (oxo), two $\mu_3$ -O (oxo), and eight $\mu_2$ -OEt groups, coordination state 6 for Ti is completed by 12 terminal OEt groups, which depict shortest Ti-O distances 1.766(6)—1.810(6) Å  |
| $\text{Nb}_8(\mu_2\text{-O})_8(\mu_3\text{-O})_2(\mu_2\text{-OEt})_6$<br>( $\text{OEt}$ ) $_{14}^{17c}$<br>( $\text{Nb}_8\text{O}_{30}$ )   | Bent/trigonal planar<br>( $\mu_2/\mu_3$ )            | 6<br>(Distorted Oh)  | $P2_1/n$       | 2 | The molecule (Figure 2) consists of eight slightly distorted $\text{NbO}_6$ octahedra and the arrangement may be visualised as two sets of three edge-sharing octahedra linked by two bridging octahedra through corner sharing, Nb-O distances vary from 2.01—2.18 Å  |

<sup>a</sup> Abbreviations Oh = Octahedral Td = Tetrahedral TBP = Trigonal bipyramidal SPyr = Square pyramidal

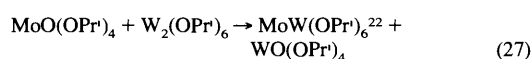
Similar to binary alkoxides, oxo-alkoxides also undergo alcoholysis reactions to afford new metal oxo-alkoxides as shown by the following reaction<sup>22</sup>



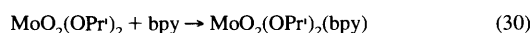
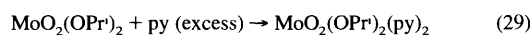
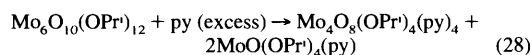
The interactions of a binary alkoxide with an oxo-alkoxide can give rise to new oxo-alkoxide derivatives



Oxo-group transfer reaction has also been observed between two different metal derivatives as exemplified by the reaction

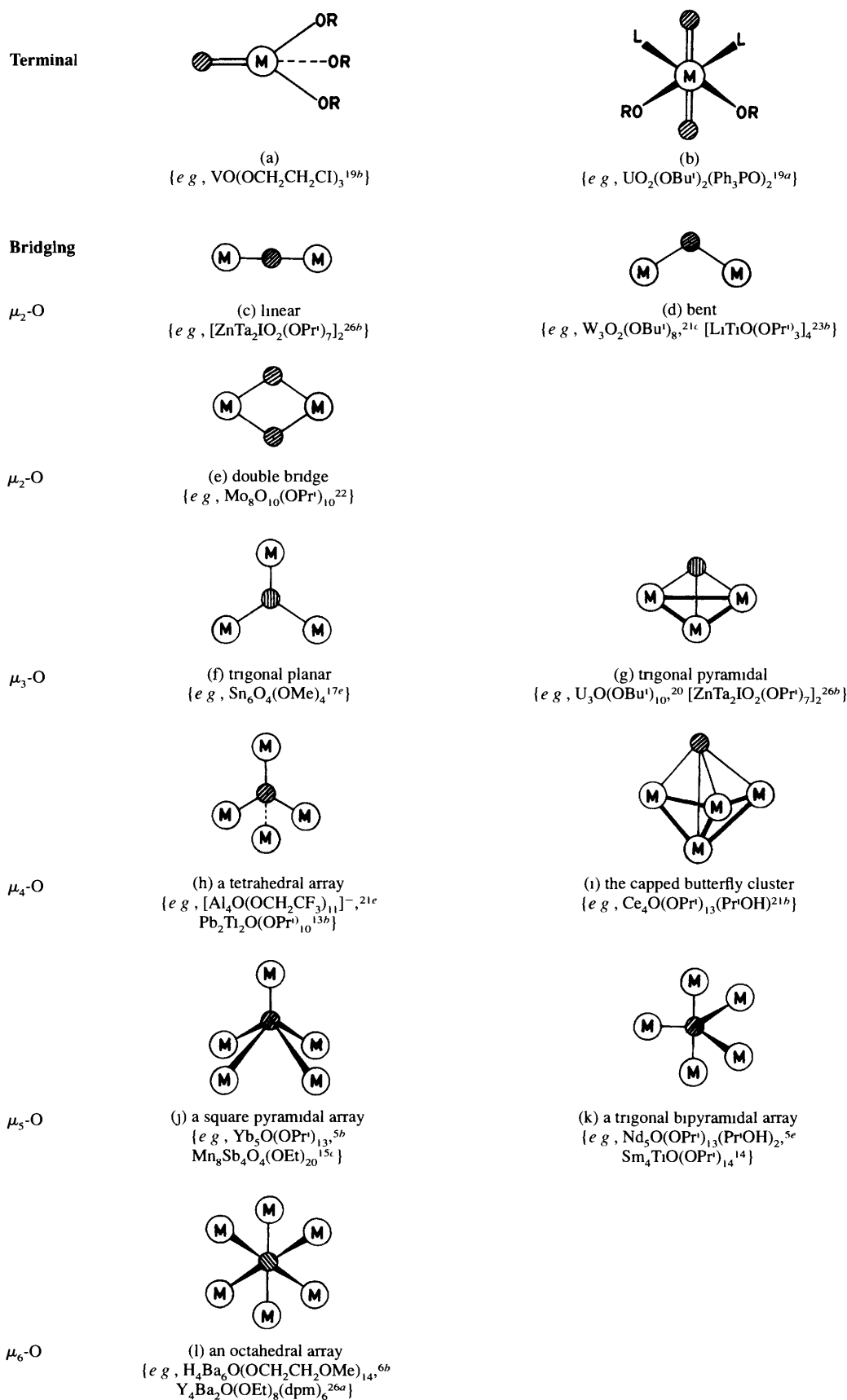


Molybdenum oxo-alkoxides also react with Lewis bases like pyridine (py) and 2,2'-bipyridyl (bpy) to form interesting addition complexes<sup>22</sup>



By contrast, derivatives  $\text{M}_5\text{O}(\text{OPr}^t)_{13}$  (M = Sc, Y, Yb) show no evidence of reactivity with Lewis bases like thf, dimethoxyethane, or py, or a Lewis acid like  $\text{Al}(\text{OPr}^t)_3$

Interestingly, the reaction between  $\text{Pb}_4\text{O}(\text{OEt})_6$  and  $\text{Nb}_2(\text{OEt})_{10}$  in ethanol forms a heterometallic oxo-alkoxide complex,  $\text{Pb}_6\text{Nb}_4\text{O}_4(\text{OEt})_{24}^{13a}$  (cf equation 13), characterized by X-ray crystallography. The formation of this complex can be viewed as the


 Figure 9 Bonding modes of oxo (O<sup>2-</sup> = ⊗) ligands

$\text{Pb}_6\text{O}(\text{OEt})_6$  unit acting as a tridentate oxo ligand towards the Lewis acid  $\text{Nb}(\text{OEt})_5$ . These types of reactions merit further exploration and extension.

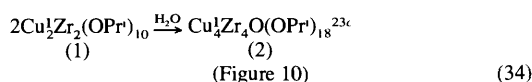
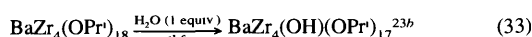
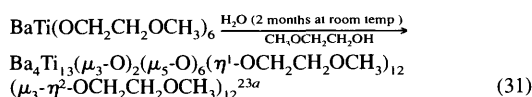
### 3 Heterometallic Oxo-alkoxides

#### 3.1 Isolation

Besides direct hydrolysis, another general route by which many bimetallic oxo-alkoxides have been synthesized consists of ester elimination from a refluxing mixture of a metal alkoxide and the carboxylate (generally acetate) of another metal. In addition to the above, the condensation reactions of a metal oxo-alkoxide with other normal metal alkoxides have also been utilized in some cases to synthesize heterometal oxo-alkoxides. These preparative routes are represented in the following sub-sections by equation(s) in the choice of which preference has been given to the latest publications as these generally incorporate earlier references also.

##### 3.1.1 Direct Hydrolytic Reactions

As emphasized in a number of publications,<sup>2,3</sup> the basic framework of a heterometal alkoxide generally remains unaltered at least in the initial stages of its hydrolysis, a pattern which assumes special significance in their applications as precursors in the sol-gel process. A few such typical reactions are illustrated below:



It is interesting that the oxidations of both (1) and (2) yield  $\text{Cu}_4^i\text{Zr}_4\text{O}_5(\text{OPr}^i)_{18}^{23c}$

Similar results have been reported from our laboratories in detailed methanolysis and hydrolysis studies of  $[\text{Mg}\{\text{Al}(\text{OPr}^i)_4\}_2]^{23d}$

##### 3.1.2 Ester Elimination Reactions

This is a method of general applicability for synthesis of heterobimetallic alkoxides of a number of metals<sup>8</sup> and even of organometallic moieties<sup>9</sup> as illustrated by the following equations:

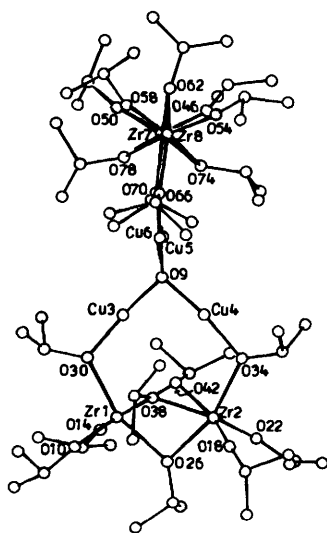
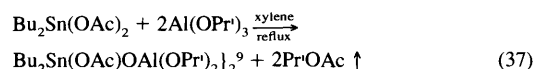
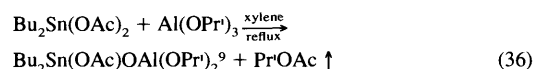
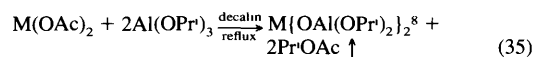
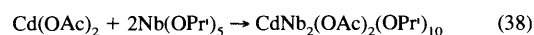


Figure 10 Molecular structure of  $\text{Cu}_4^i\text{Zr}_4\text{O}(\text{OPr}^i)_{18}^{23c}$



The role of a coordinating solvent like pyridine in leading to ligand exchange rather than ester elimination reactions between  $\text{Sn}(\text{OBu}^t)_4$  and  $\text{Sn}(\text{OAc})_4/\text{Me}_3\text{Si}(\text{OAc})$  in a hydrocarbon solvent has been mentioned earlier<sup>10</sup> (*cf.* Section 1).

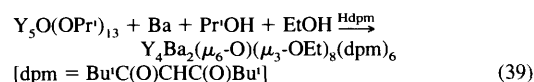
Even in hydrocarbon solvents (*e.g.*, toluene), contrary to the ester elimination reaction occurring generally in such systems,<sup>8-11,24</sup> the formation of an addition product,  $\text{Nb}_2\text{Cd}(\mu\text{-OAc})_2(\mu\text{-OPr}^i)_4(\text{OPr}^i)_6$  has been reported<sup>25a</sup> from  $\text{Nb}(\text{OPr}^i)_5$  and  $\text{Cd}(\text{OAc})_2$ :



Obviously, the role of solvent and other factors, *e.g.* molecular association of the alkoxide, requires further investigations.

##### 3.1.3 Condensation Reactions between Oxo- and Normal Metal Alkoxides

As in the commonly utilized route for synthesis of bimetallic alkoxides, heterometallic oxo-alkoxides have been synthesized by the condensation of component alkoxides and oxo-alkoxides as illustrated by a few examples<sup>12,13</sup> in Section 1. In view of the importance of Y-Ba precursors for 1,2,3 superconductors, a novel barium yttrium oxo-alkoxide,  $[\text{Y}_4\text{Ba}_2(\mu_6\text{-O})(\mu_3\text{-OEt})_8(\text{dpm})_6]$  (Figure 11), has been synthesized<sup>26a</sup> by the following reaction:



##### 3.1.4 Reactions between Metal Halides and Alkali Alkoxo-metallates

This type of reaction which has been utilised<sup>1</sup> extensively for synthesis of heterometallic normal alkoxides has been reported (*cf.* Section 1) for heterometal oxo-alkoxides also in some cases, *e.g.*, the reaction between  $\text{SmI}_2$  and  $\text{NaTi}(\text{OPr}^i)_5$  yields<sup>14</sup>  $[\text{Sm}_4\text{Ti}(\mu_5\text{-O})(\mu_3\text{-OPr}^i)_2(\mu\text{-OPr}^i)_6(\text{OPr}^i)_6]$  (Figure 12), which could also be isolated by the reaction between  $\text{Sm}_5\text{O}(\text{OPr}^i)_3$  and  $\text{Ti}(\text{OPr}^i)_4$ .

Similarly, the reaction at room temperature between  $\text{ZnI}_2$  and

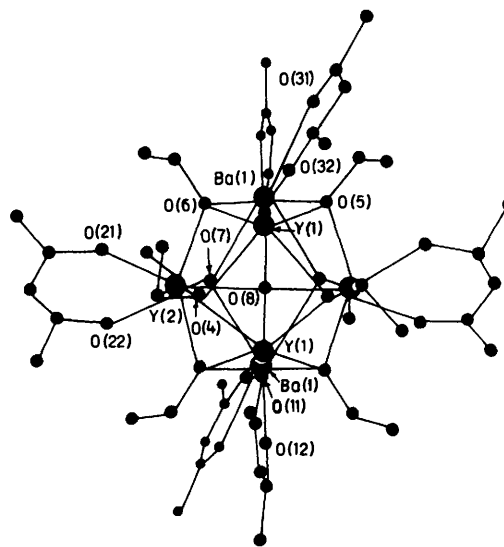


Figure 11 Molecular structure of  $[\text{Y}_4\text{Ba}_2\text{O}(\text{OEt})_8(\text{dpm})_6]^{26a}$



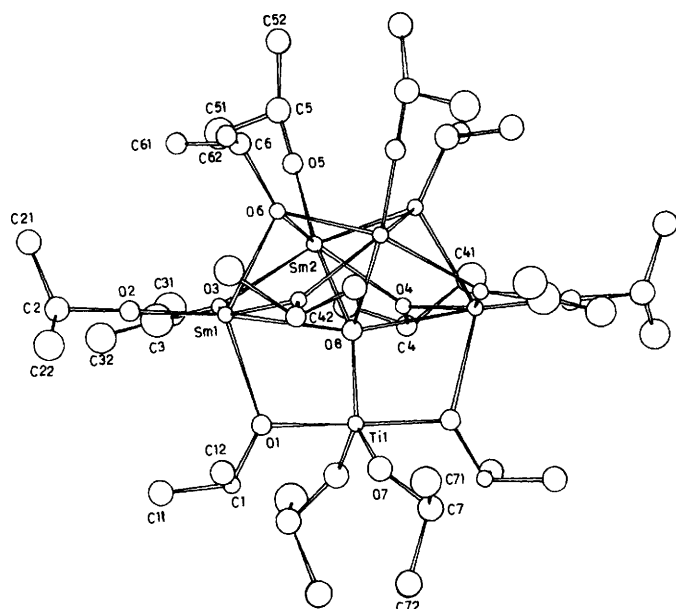


Figure 12 Molecular structure of  $\text{Sm}_4\text{TiO}(\text{OPr})_{14}$ .<sup>14</sup>

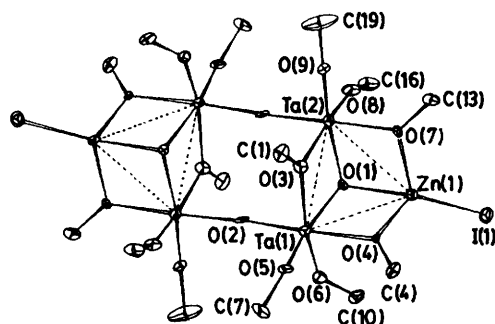
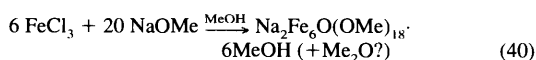


Figure 13 Molecular structure of  $[\text{ZnTa}_2\text{IO}_2(\text{OPr})_7]$ .<sup>26b</sup>

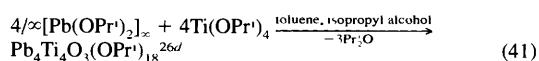
$\text{KTa}(\text{OPr}^i)_6$  (1:2 stoichiometry) in thf yielded<sup>26b</sup>  $\text{ZnTa}_2\text{O}_2(\text{OPr}^i)_8$ . Although the crystal structure of this product could not be elucidated, the structure of the intermediate derivative,  $[\text{ZnTa}_2\text{I}(\mu_3\text{-O})(\mu_2\text{-O})(\mu\text{-OPr}^i)_3(\text{OPr}^i)_4]_2$ , obtained by the 1:1 reaction of  $\text{ZnI}_2$  with  $\text{KTa}(\text{OPr}^i)_6$  can be represented by Figure 13.

Another interesting  $\mu_6$ -oxo-centred iron(III) heterometal methoxide derivative  $\text{Na}_2\text{Fe}_6\text{O}(\text{OMe})_{18} \cdot 6\text{MeOH}$  had been reported<sup>26c</sup> earlier by the reaction between iron(III) chloride and sodium methoxide:

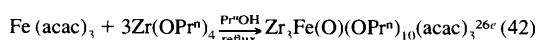


### 3.1.5 Other Methods for Synthesis of Heterometallic Oxo-alkoxide Derivatives

In addition to the condensation of a metal oxo-alkoxide with the alkoxide of another metal (Section 3.1.3), the interaction of normal alkoxides of two metals also under some (so far not fully understood) conditions yields a heterometal oxo-alkoxide, *e.g.*,



Similarly, the condensation of an acetylacetonato-metal with the normal alkoxide of another metal leads to a heterometal oxo-alkoxide acetylacetonato (acac) derivative, *e.g.*:



## 3.2 Spectroscopic Properties

Salient features of the applications of spectroscopic (IR, NMR) techniques to the study of heterometallic oxo-alkoxide derivatives are similar to those already described in Section 2.2 for homometallic oxo-alkoxide species.

Routine IR data have been reported<sup>8,9,13a,b,14,15b,23c,d,24a,d</sup> for most of the derivatives which showed the presence of alkoxo groups in addition to oxo and acac moieties if present. Appearance of new bands in the region  $700\text{--}400 \text{ cm}^{-1}$  provides evidence for both the presence of metal–oxygen bonds and the heterometallic nature of the species.

An increasing number of NMR studies<sup>8,9,13a,b,14a,23a,b,25b,26a,b</sup> of metal oxo-alkoxides in solution give general information, *e.g.*, environments around metal atoms, ligating modes of oxo- and alkoxo-ligands, and this information complements the X-ray data in a number of cases. Further NMR ( $^1\text{H}$ ,  $^{13}\text{C}$ ) studies have shown evidence of alkoxo ligand exchange (*e.g.*, fluxional behaviour) in derivatives like  $[\text{ZnTa}(\mu_3\text{-O})(\mu_2\text{-O})(\mu_2\text{-OPr}^i)_3(\text{OPr}^i)_4]_2$ <sup>26b</sup> and  $\text{Pb}_2\text{Ti}_2(\mu_4\text{-O})(\mu_3\text{-OPr}^i)_2(\mu_2\text{-OPr}^i)_4(\text{OPr}^i)_4$ <sup>13b</sup> and a rigid structure in  $\text{Sm}_4\text{Ti}(\mu_5\text{-O})(\mu_3\text{-OPr}^i)_2(\mu_2\text{-OPr}^i)_6(\text{OPr}^i)_6$ .<sup>14</sup> Examples are also known of derivatives like  $\text{Pb}_6\text{Nb}_4\text{O}_4(\text{OEt})_{24}$ <sup>13a</sup> and  $[\text{PbZr}_2\text{O}(\text{OAc})_2(\text{OEt})_6]_2$ <sup>25b</sup> which dissociate in solution, as evidenced by the complex nature of their spectra.

$^{207}\text{Pb}$  NMR investigations have provided information<sup>13a,25b,26d</sup> about the coordination number of the metal atoms and their environments.

## 3.3 X-Ray Crystallographic Studies

The generalization, that the degree of association ‘*a*’ in simple binary alkoxides  $[\text{M}(\text{OR})_n]_a$  tends to be the lowest for the attainment of the requisite coordination state of the central metal, appears to be operative in the case of heterometal alkoxides  $\text{M}_x\text{M}'_y(\text{OR})_z$ , with the value of  $z/(x+y)$  typically being low. The replacement of two alkoxo ( $-\text{OR}$ ) groups by an oxo ( $\text{O}^{2-}$ ) ligand with higher bridging functionality also appears to be preferred for keeping the molecular structure as condensed as possible.

Structures of heterometal oxo-alkoxides also are, therefore, based on the same types of bonding modes of  $\text{O}^{2-}$  ligands as described in Section 2.3; a few typical examples are included in Table 2 and four of these are illustrated in Figures 10–13.

## 3.4 Reactions

Work on heterometallic oxo-alkoxides appears to be limited to the isolation and structural characterization of bimetallic derivatives. However, there appears to be no publication dealing with their chemical reactivity. The condensation of these bimetallic derivatives with alkoxides/oxo-alkoxides of other metals could be further investigated<sup>11</sup> for synthesis of higher heterometallic derivatives. Further, the structural changes brought about in the bimetallic oxo-alkoxide framework on replacement of all or some of the alkoxo groups by more highly functionalized or chelating alkanols– $\beta$ -diketones, *etc.*, should throw revealing light on their stability and lead to a better understanding about their isolation, which in many cases remains sporadic so far.

## 4 Mechanism (Hydrolytic and Non-hydrolytic) for the Formation of Oxo-alkoxide Derivatives

Starting with the work of Bradley *et al.*<sup>1</sup> on a number of systems, the synthesis of many oxo-alkoxide derivatives by direct hydrolysis of homo- and hetero-metal alkoxides has been described in Sections 2.1.2 and 3.1.1, respectively.

NMR ( $^{29}\text{Si}$  and  $^{17}\text{O}$ ) spectroscopy has been extensively employed during the last few years to elucidate the mechanism of hydrolysis of alkoxides of silicon and titanium. A special mention may be made of the ‘building block’ approach by Klemperer and coworkers,<sup>27a</sup> who suggested the role of  $[\text{Si}_8\text{O}_{12}](\text{OMe})_x$  with a comparatively more rigid  $\text{Si}_8\text{O}_{12}$  core than the expected lower

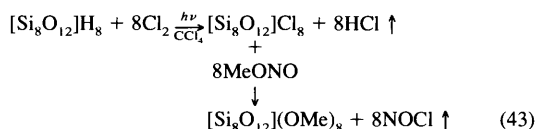
**Table 2** X-Ray structural data for a few typical heterometallic oxo-alkoxide derivatives

| Compound<br>(Metal oxygen core)   | Geometry of the<br>oxo ligand and<br>(Bridging mode) | Coordination<br>number<br>(Geometry)<br>of the metal            | Space<br>group | Z | Comments   |
|---|--|---|----------------|---|--|
| $\text{Pb}_2\text{Tl}_2(\mu_4\text{-O})(\mu_3\text{-OPr})_2$<br>$(\mu_2\text{-OPr})_4(\text{OPr})_4^{13b}$<br>$(\text{Pb}_2\text{Tl}_2\text{O}_{11})$                                 | Severely distorted Td<br>( $\mu_4$ )                 | Tl 6<br>(Distorted Oh)<br>Pb 5<br>(Distorted TBP)               | $P2_1/n$       | 4 | Tl–O and Pb–O distances vary from 1.80(1) to 2.20(1) Å and 2.33(1) to 2.51(1) Å, respectively, terminal Tl–O–C angles are large 136(1) to 166(2)°  |
| $\text{Sm}_4\text{Tl}(\mu_5\text{-O})(\mu_3\text{-OPr})_2$<br>$(\mu_2\text{-OPr})_6(\text{OPr})_6^{14}$<br>$(\text{Sm}_4\text{TlO}_{15})$   | TBP<br>( $\mu_5$ )                                   | Sm 6<br>(Oh)<br>Tl 5<br>(Distorted TBP)                         | $I4_1cd$       | 8 | The molecular structure (Figure 12) is a pentanuclear oxo species with an encapsulated $\mu_5$ -oxo ligand, Sm–O distances vary from 2.04(2) to 2.699(4) Å, the order of variation being terminal $< \mu_2 \approx \mu_3 < \mu_5$ , the Tl–O distances are shorter [1.81(2)—1.98(2) Å]   |
| $[\text{ZnTa}_2\text{I}(\mu_3\text{-O})(\mu_2\text{-O})$<br>$(\mu_3\text{-OPr})_3(\text{OPr})_4]^{26b}$<br>$(\text{Zn}_2\text{Ta}_2\text{O}_{18})$                                    | Trigonal pyramidal/<br>linear<br>( $\mu_3/\mu_2$ )   | Ta 6<br>(Distorted Oh)<br>Zn 4<br>(Distorted Td)                | $P2_1/c$       | 2 | The centrosymmetric dimer derivative (Figure 13) consists of two triangular $\text{Ta}_2\text{Zn}(\mu_3\text{-O})(\mu_2\text{-OPr})_3$ I units linked by two oxo bridges, involving the two Ta centres of both units, Ta–O–Ta oxo bridges are almost linear (175.30°), Ta–O and Zn–O distances vary from 1.83(1) to 2.12(1) Å and 1.95(1) to 2.10(1) Å, respectively   |
| $\text{Y}_4\text{Ba}_2(\mu_6\text{-O})(\mu_3\text{-OEt})_8$<br>$(\text{dpm})_6^{26a}$<br>[dpm = Bu <sup>t</sup> C(O)CHC(O)Bu <sup>t</sup> ]<br>$(\text{Y}_4\text{Ba}_2\text{O}_{21})$ | Oh<br>( $\mu_6$ )                                    | Ba 7<br>Y 7   | $P\bar{1}$     | 1 | The crystal structure (Figure 11) consists of an oxygen-centred octahedron built up from two barium and four yttrium atoms linked by eight $\mu_3$ -OEt groups, each of which is chelated by a terminal dpm ligand to give a coordination of 7 for both Ba and Y atoms, the observation that Ba–O–C(Et) angles (av. 110.3°) are smaller than the Y–O–C(Et) (126.8°) indicates that the $\pi$ -donation from the OEt groups is more significant to Y than to Ba atoms   |
| $[\text{LiTiO}(\text{OPr})_3]_4^{23b}$<br>$(\text{Li}_4\text{Ti}_4\text{O}_{16})$   | Bent/TBP<br>( $\mu_2/\mu_5$ )                        | Ti 6/5<br>(Oh/Distorted TBP)<br>Li 4<br>(Very unusual geometry) | $C2/c$         | 4 | The molecule has neither a crystallographic proper axis of rotation nor a mirror plane, but possesses crystallographic $C_2$ symmetry, the structure of the central portion consists of a double (face-shared) cube of formula $\text{Li}_4\text{Ti}_2\text{O}_2(\text{OPr})_{10}^{2-}$ , with two oxo- $\text{TiO}(\text{OPr})^+$ groups, the four oxo ligands adopt $\mu_2$ - and $\mu_5$ -structural patterns, the observed Ti–O distances, are in the order terminal $\text{Ti–OPr}^+ < \mu_2\text{-OPr}^+ < \mu_5\text{-O}$ |
| $\text{Na}_2\text{Fe}_6(\mu_6\text{-O})(\mu_2\text{-OMe})_{12}$<br>$(\text{OMe})_6$ 6MeOH <sup>26c</sup><br>$(\text{Na}_2\text{Fe}_6\text{O}_{25})$                                   | Oh<br>( $\mu_6$ )                                    | Na 6<br>(Oh)<br>Fe 6<br>(Distorted Oh)                          | $P4_22_2$      | 4 | The $\mu_6$ -oxo ligand is in the centre of an octahedron of six Fe atoms, which are themselves connected to each other by 12 $\mu_6$ -OMe bridges and each Fe centre is linked with one terminal OMe group, each of the two Na <sup>+</sup> ions, is linked to three OMe bridges of the $\text{OFe}(\text{OMe})_6$ moiety and to three additional MeOH molecules  |
| $\text{Cu}_4\text{Zr}_4(\mu_4\text{-O})(\mu_2\text{-OPr})_{10}$<br>$(\text{OPr})_8^{23c}$<br>$(\text{Cu}_4\text{Zr}_4\text{O}_{20})$  | Distorted Td<br>( $\mu_4$ )                          | Zr 6<br>(Oh)<br>Cu 2<br>(Linear)                                | $P2_1/c$       | 8 | The molecule (Figure 10) consists of two $\text{Cu}_2\text{Zr}_2(\text{OPr})_9^+$ fragments linked through the four Cu centres via a pseudo-tetrahedral oxo ligand, the copper atoms are bridged by an oxo ligand giving the metal centres a two-coordinate linear geometry (172.9° av)  |
| $\text{Pb}_6\text{Nb}_4(\mu_4\text{-O})_4(\mu_3\text{-OEt})_4$<br>$(\mu_2\text{-OEt})_{12}(\text{OEt})_8^{13a}$<br>$(\text{Pb}_6\text{Nb}_4\text{O}_{28})$                            | Distorted Td<br>( $\mu_4$ )                          | Nb 6<br>(Oh)<br>Pb 6<br>(Distorted trigonal prismatic)          | $P2_1/n$       | 4 | The X-ray structure of the decanuclear complex shows an octahedral $\text{Pb}_6$ framework, four of the faces of which are capped by a $\mu_4$ -oxo ligand connected to a $\text{Nb}(\text{OEt})_5$ moiety and to three Pb atoms, the remaining faces of the Pb octahedron are capped by $\mu_3$ -OEt groups, Pb–O   |

Table 2 contd

| Compound<br>(Metal oxygen core)  | Geometry of the<br>oxo ligand and<br>(Bridging mode) | Coordination<br>number<br>(Geometry)<br>of the metal | Space<br>group | Z | Comments   |
|--|--|--|----------------|---|--|
| $\text{Mn}_8\text{Sb}_4(\mu_4\text{-O})_4(\mu_3\text{-OEt})_4$<br>( $\mu_3\text{-OEt}$ ) <sub>16</sub> <sup>15c</sup><br>( $\text{Mn}_8\text{Sb}_4\text{O}_{24}$ )   | Distorted SPYr<br>( $\mu_3$ )                        | Mn: 6/5<br>(Distorted Oh/SPYr)                       | $C2/c$         | 4 | distances follow the pattern $\mu_4\text{-O} < \mu_3\text{-OEt} < \mu_2\text{-OEt}$ with values ranging from 2.28(8) to 3.1(1) Å.<br><br>The packing of the dodecanuclear globular shaped molecules can be approximately viewed as a body-centred cube, with an approximately $S_4$ symmetry; $\text{Sb}^{\text{III}}$ atoms are five-coordinated; four of the $\text{Mn}^{\text{II}}$ atoms are octahedrally coordinated, while the remaining four are five-coordinated.  |
| $\text{Ba}_4\text{Ti}_{13}(\mu_3\text{-O})_{12}(\mu_5\text{-O})_6$<br>( $\mu_1\text{-}\eta^1\text{-OCH}_2\text{CH}_2\text{OCH}_3$ ) <sub>12</sub><br>( $\mu_1, \mu_3\text{-}\eta^2\text{OCH}_2\text{CH}_2\text{OCH}_3$ ) <sub>2</sub> <sup>23a</sup><br>( $\text{Ba}_4\text{Ti}_{13}\text{O}_{54}$ ) | T-shaped/TBP<br>( $\mu_3/\mu_5$ )                    | Ba: 12<br>Ti: 6<br>(Distorted Oh)                    | $C2/c$         | 4 | Molecular structure of the barium titanium oxo-alkoxide revealed a tetrahedron of $\text{BaO}_3$ units superimposed on a $\text{TiO}_6(\text{TiO}_3)_{12}$ core; each Ba atom is linked with 6 oxo ligands and 6 oxygen atoms from 3 chelating methoxyethoxy ligands; the central Ti atom is octahedrally coordinated to 6 trigonal-bipyramidal oxo ligands, while the external Ti atoms are coordinated to one internal $\mu_3$ -oxo ligands in addition to one terminal ( $\eta^1$ ) and two bridging ( $\mu_3\text{-}\eta^2$ ) alkoxide oxygen atoms. |

building blocks like  $[\text{Si}_2\text{O}](\text{OMe})_6$  and  $[\text{Si}_3\text{O}_2](\text{OMe})_8$  in the hydrolysis of  $\text{Si}(\text{OMe})_4$  by the sol-gel process. The synthesis of  $[\text{Si}_8\text{O}_{12}](\text{OMe})_8$  had been described<sup>27b</sup> earlier by the following reactions:

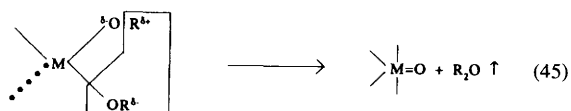


Using <sup>17</sup>O enriched H<sub>2</sub>O and taking into account the kinetic inertness of the C–O bonds during the hydrolysis of  $\text{Ti}(\text{OPr})_4$  in  $\text{Pr}^i\text{OH-MeOH}$ , Klemperer *et al.*<sup>27c</sup> were able to identify the formation of a number of oxo-alkoxide species as a result of the overall reaction:



The species with the lowest value of  $y/x = 0.33$ , i.e.,  $[\text{Ti}_3\text{O}](\text{OPr})_9(\text{OMe})$  was found to be extremely unstable, whereas the species with the  $[\text{Ti}_{16}\text{O}_{16}]$  core was shown to be the most stable and resistant to further hydrolysis; this last species appears to be retained in the initial stages of the sol-gel polymerization of titanium alkoxides.

In addition to the straightforward hydrolysis reactions, a considerable amount of evidence has accumulated, as mentioned in Section 1 also, on the nonhydrolytic conversion of alkoxides into oxo-alkoxides and different plausible mechanisms have been suggested. For example, Tuvova *et al.*<sup>4</sup> have recently shown that the decomposition of  $\text{MoO}(\text{OEt})_4$ ,  $\text{MoO}(\text{OPr})_4$  (especially when freshly prepared),  $\text{W}(\text{OEt})_6$  and  $\text{Cs}\{\text{Nb}(\text{OPr})_n\text{F}_{6-n}\}$  occurs with the elimination of ether molecules to form oxo-alkoxide derivatives, e.g.:

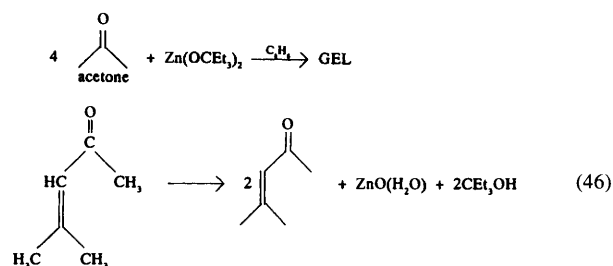


Ether elimination appears to be involved also during the formation of  $\text{Pb}_4\text{Ti}_4\text{O}_3(\text{OPr})_8$ <sup>26d</sup> by the condensation of isopropoxides of lead and titanium.

An alternative route of conversion of di-tertiary and -secondary alkoxides into oxo-alkoxides by elimination (as shown by mass spectroscopy) of small amounts of alkenes (with parent alcohols) or the ketone, e.g.,  $(\text{Me}_3\text{C})_2\text{C}=\text{O}$  respectively has been shown to occur<sup>16</sup> when attempts are made to sublime alkoxides of barium, such as  $\text{Ba}(\text{OCeEt}_3)_2$ ,  $\text{Ba}(\text{OCMeEtPr}^i)_2$ ,  $\text{Ba}(\text{OCMe}_3)_2$ , and  $\text{Ba}\{\text{OCH}(\text{CMe}_2)_2\}_2$ .

Although the full mechanism could not so far be elucidated, the conversion of  $\text{KZr}_2(\text{OPr}^i)_9$  into  $\text{K}_4\text{Zr}_2\text{O}(\text{OPr}^i)_{10}$  has been proposed<sup>26f</sup> to involve the fission of C–O bonds of the isopropoxide groups,  $\text{Me}_2\text{C}(\text{H})-\text{O}$ , yielding  $(\text{Me}_2\text{CH}_2)$  and the oxo-zirconium derivative,  $\text{K}_4\text{Zr}_2\text{O}(\text{OPr}^i)_{10}$ .

Employing acetone as a condensing reagent, the conversion of the hydrocarbon-soluble  $\text{Zn}(\text{OCeEt}_3)_2$  to a rigid transparent gel, followed by conversion to ZnO by an aldol condensation-elimination sequence has been shown<sup>28</sup> to occur *via* the following plausible mechanism:



Briefly, a number of possible mechanisms have been proposed for the formation of oxo-alkoxides in an increasing number of apparently anhydrous systems. In fact, the possibility of different mechanisms being simultaneously operative under such diverse conditions cannot be ruled out. Obviously, much more directed and quantitative investigations are called for to arrive at an integrated view of the problem, which could lead to predictions on possibilities of a more effective control of the optimum conditions for obtaining a desired oxo-alkoxide in the maximum yield.

## 5 A Comparison of the Oxo-alkoxide Derivatives with Metal Alkoxides and Oxides

Oxo-alkoxides of metals obviously constitute an interesting series of intermediates between alkoxides and oxides of metals. Chisholm<sup>29</sup> has predicted that 'metal alkoxides may act as models for metal oxides in their reactions with a wide variety of hydrocarbons and small unsaturated molecules'. It has been pointed out<sup>29</sup> that the central  $Ti_7O_{24}$  and  $Nb_8O_{10}$  core units in  $Ti_7O_4(OEt)_{20}$  and  $Nb_8O_{10}(OEt)_{20}$  (Figures 1 and 2) respectively reveal a striking similarity to both the structure of  $Ti(OEt)_4$  as well as those of iso- and hetero-polyacids of vanadium and molybdenum. More and more such similarities are emerging in the structures (Figures 1–13) of metal oxo-alkoxides which are in between those of alkoxides and oxides of the corresponding metals.

## 6 Potential Applications and Future Developments

In view of their volatility, solubility in organic solvents, ease of purification and facile hydrolysis, binary as well as heterometallic alkoxides and oxo-alkoxides are emerging as extremely attractive precursors<sup>2,3,30</sup> for the preparation of ceramic materials by the sol-gel<sup>30a</sup> as well as by the metal-organic chemical vapour deposition (MOCVD)<sup>30b</sup> processes.

In spite of highly attractive features, the applications of alkoxo derivatives of metals as precursors for ceramic materials has been limited by the difficulty in handling them owing to their extremely high sensitivity to hydrolysis even by traces of atmospheric moisture. The corresponding oxo-alkoxides are comparatively less sensitive to such hydrolytic processes and can, therefore, be handled with less difficulty.

The preformed heterometallic alkoxides are now generally preferred<sup>31</sup> to a mixture of component alkoxides as they tend to yield finally a more homogeneous material. The atomic ratio of different metals (e.g. Pb/Ti) can be 1:1 as required for lead titanate,  $PbTiO_3$  perovskite, which is a desirable ferroelectric material, the use of such 'single source' precursors<sup>31</sup> as  $Pb_2Ti_2(\mu_2-O)(\mu_3-OPr)_2(\mu-OPr)_4(OPr)_4$ <sup>13b</sup> thus offers a distinct advantage for obtaining ceramic materials.

In addition to their rapidly emerging applications<sup>30b</sup> for preparation of ceramic materials, bimetallic  $\mu$ -oxo-alkoxides with the general formula,  $(RO)_n-M'-O-M''-OM'(OR)_{n-1}$  (where  $M' = Al$  or  $Ti$  with  $n = 3$  and  $4$  respectively and  $M''$  is a bivalent metal such as Mn, Fe, Co, Ni, Zn and  $R = Pr$  or  $Bu$ ) are amongst the most promising catalysts for polymerization of heterocyclic monomers, such as lactones, oxiranes and epoxides.<sup>8</sup> Further, dimeric alkoxides of Mo and W, generally with metal-metal bonds, have been shown<sup>29</sup> to be effective catalysts for reactions like alkyne polymerization and alkene isomerization.

Concerted efforts initiated recently to elucidate the basic chemistry of the manifold applications of oxo-alkoxides are enhancing the efficacy of such applications. Besides the above, the synthesis of a large number of stable heterometal oxo-alkoxides with alkoxo and oxo bridges between different metals has added a new dimension to our understanding of mixed-metal coordination chemistry. Further, the isolation of an increasing number of homo- as well as hetero-metallic oxo-alkoxides with compact structures involving  $\mu_2$ - to  $\mu_6$ -O ligands shows many novel features, which merit further study from both the theoretical as well as the synthetic point of view.

**Acknowledgments** The authors thank the Department of Science and Technology, New Delhi, for continued financial support of their work.

## 7 References

- (a) D C Bradley, R C Mehrotra, and D P Gaur, 'Metal Alkoxides', Academic Press, London, 1978, pp 150–167, (b) D C Bradley, *Philos Trans R Soc London*, 1990, **A330**, 167
- (a) R C Mehrotra, in 'Sol Gel Science and Technology', eds M A Aegerter, M Jafelicci Jr., D F Souza and F D Zanotto, World Scientific, Singapore, 1989, pp 27–31, (b) R C Mehrotra, 'Present Status and Future Potential of the Sol-Gel Process', in 'Chemistry, Spectroscopy and Applications of Sol-Gel Glasses', eds R Reisfeld and C K Jorgensen, Springer Verlag, Berlin, 1992, pp 1–36
- C J Brinker and G W Scherer, 'Sol-Gel Science—The Physics and Chemistry of Sol-Gel Processing', Academic Press, Inc., San Diego and London, 1990, pp 21–96 (non silicates) and 97–234 (silicates)
- N Ya Turova, V G Kessler and S I Kucheiko, *Polyhedron*, 1991, **10**, 2617, V G Kessler, N Ya Turova and A Panov, *Polyhedron*, 1996, **15**, 335
- (a) O Poncelet, W J Sartain, L G Hubert Pfalzgraf, K Foltung and K G Caulton, *Inorg Chem*, 1989, **28**, 263, (b) D C Bradley, H Chudzynska, D M Frigo, M E Hammond, M B Hursthouse and M A Mazid, *Polyhedron*, 1990, **9**, 719, (c) O Helgesson, S Jagner, O Poncelet and L G Hubert Pfalzgraf, *Polyhedron*, 1993, **12**, 1411, (d) R C Mehrotra, *Chemtracts*, 1990, **2**, 143
- (a) K G Caulton, M H Chisholm, S R Drake and K Foltung, *J Chem Soc Chem Commun*, 1990, 1349, (b) K G Caulton, M H Chisholm, S R Drake and J C Huffman, *J Chem Soc Chem Commun*, 1990, 1498
- N Ya Turova, E P Turevskaya, V G Kessler, A I Yanovsky and Yu T Struchkov, *J Chem Soc Chem Commun*, 1993, 21
- Sonika, A K Narula, O P Vermani and H K Sharma, *J Organometal Chem*, 1994, **470**, 67 and references therein
- J Rai and R C Mehrotra, *J Non Cryst Solids*, 1991, **134**, 23
- (a) J Caruso, M J Hampden Smith, A L Rheingold and G Yap, *J Chem Soc Chem Commun*, 1995, 157, (b) J Caruso, C Roger, F Schwertfeger, M J Hampden Smith, A L Rheingold and G Yap, *Inorg Chem*, 1995, **34**, 449
- R C Mehrotra and coworkers, unpublished results
- A I Yanovsky, M I Yanovskaya, V K Limar, V G Kessler, N Ya Turova and Yu Struchkov, *J Chem Soc Chem Commun*, 1991, 1605
- (a) R Papiernik, L G Hubert Pfalzgraf, J C Daran and Y Jeannin, *J Chem Soc Chem Commun*, 1990, 695, (b) S Daniele, R Papiernik, L G Hubert-Pfalzgraf, S Jagner and M Hakansson, *Inorg Chem*, 1995, **34**, 628
- S Danielle, L G Hubert Pfalzgraf, J C Daran and S Halut, *Polyhedron*, 1994, **13**, 927
- (a) U Bemm, R Norrestam, M Nygren and G Westin, *Inorg Chem*, 1992, **31**, 2050 (b) U Bemm, K Lashgari, R Norrestam, M Nygren and G Westin, *J Solid State Chem*, 1994, **108**, 243, (c) U Bemm, R Norrestam, M Nygren and G Westin, *Inorg Chem*, 1995, **34**, 2367
- (a) A Purdy, C F George and J H Callahan, *Inorg Chem*, 1991, **30**, 2812 (b) R C Mehrotra, A Singh and S Sogani, *Chem Soc Rev*, 1994, **23**, 215
- (a) K Watenpaugh and C N Caughlan, *Chem Commun*, 1967, 76, (b) R Schmid, A Mosset and J Galy, *J Chem Soc Dalton Trans*, 1991, 1999, (c) D C Bradley, M B Hursthouse and P F Rodesler, *J Chem Soc Chem Commun*, 1968, 1112, (d) B Morrison, *Crystallogr Sect B*, 1977, **33**, 303, (e) P G Harrison, B J Haylett and J King, *J Chem Soc Chem Commun*, 1978, 112
- C Lambert, F Hampel, P v R Schleyer, M G Davidson and R Snath, *J Organomet Chem*, 1995, **487**, 139
- (a) C J Burns, D C Smith, A P Sattelberger and H B Gray, *Inorg Chem*, 1992, **31**, 3724, (b) W Priebsch and D Rehder, *Inorg Chem*, 1990, **29**, 3013, (c) D C Crans, H Chen and R A Felty, *J Am Chem Soc*, 1992, **114**, 4543
- F A Cotton, D O Marler and W Schwotzer, *Inorg Chim Acta*, 1984, **95**, 207
- (a) S Doeuff, Y Dromzee, F Taulelle and C Sanchez, *Inorg Chem*, 1989, **28**, 4439, (b) K Yunlu, P S Gradedff, N Edelstein, W Kot, G Shalimoff, W E Strieb, B A Vaarstra and K G Caulton, *Inorg Chem*, 1991, **30**, 2317, (c) T P Blatchford, M H Chisholm, K Foltung and J C Huffman, *J Chem Soc Chem Commun*, 1984, 1295 (d) M H Chisholm, C M Cook and K Foltung, *J Am Chem Soc*, 1992, **114**, 2721, (e) S A Sangokoya, W T Pennington, J Byers Hill and G H Robinson, *Organometallics*, 1993, **12**, 2429
- M H Chisholm, K Foltung, J C Huffman and C C Kirkpatrick, *Inorg Chem*, 1984, **23**, 1021
- (a) J F Campion, D A Payne, H K Chal, J K Maurin and S R Wilson, *Inorg Chem*, 1991, **30**, 3244, (b) R Kuhlman, B A Vaarstra, W E Streib, J C Huffman and K G Caulton, *Inorg Chem*, 1993, **32**, 1272, (c) J A Samuels, W C Chiang, J C Huffman, K L Trojan, W E Hatfield, D V Baxter and K G Caulton, *Inorg Chem*, 1994, **33**, 2167 (d) J Rai and R C Mehrotra, *J Non Cryst Solids*, 1993, **152**, 118
- K G Caulton and L G Hubert Pfalzgraf, *Chem Rev*, 1990, **90**, 969
- S Boulmaaz, R Papiernik and L G Hubert Pfalzgraf, *Chem Mater*, 1991, **3**, 779
- (a) P Miele, J D Foulon, N Hovnanian and L Cot, *J Chem Soc Chem Commun*, 1993, 29, (b) S Boulmaaz, L G Hubert Pfalzgraf, S Halut and J C Daran, *J Chem Soc Chem Commun*, 1994, 601 (c)

- K. Hegetschweiler, H. W. Schmalte, H. M. Streit, V. Gramlich, H. U. Hund and I. Erni, *Inorg. Chem.*, 1992, **31**, 1299; (d) R. Papiernik, L. G. Hubert-Pfalzgraf and F. Chaput, *J. Non-Cryst. Solids*, 1992, **147**, 36; (e) R. Schmid, H. Ahamdane and A. Mosset, *Inorg. Chim. Acta*, 1991, **190**, 237; (f) B. A. Vaarstra, W. E. Streib and K. G. Caulton, *J. Am. Chem. Soc.*, 1990, **112**, 8593.
- 27 (a) Y. W. Chen, W. G. Klemperer and C. W. Park, *Mater. Res. Soc. Symp. Proc.*, 1992, **271**, 57; (b) V. W. Day, W. G. Klemperer, V. V. Mainz and D. M. Millan, *J. Am. Chem. Soc.*, 1985, **107**, 8262; (c) Y. Chen, J. Hao, W. G. Klemperer, C. W. Park and F. S. Rosenberg, *Polym. Preprint. Am. Chem. Soc. Div. Polym. Chem.*, 1993, **34**, 250.
- 28 S. C. Goel, M. Y. Chiang, P. C. Gibbons and W. E. Buhro, *Mater. Res. Soc. Symp. Proc.*, 1992, **271**, 3.
- 29 M. H. Chisholm, in 'Inorganic Chemistry: Toward the 21st Century', ed. M. H. Chisholm, *Am. Chem. Soc.*, Washington, DC, 1982, pp. 243—268.
- 30 (a) D. C. Bradley, *Polyhedron*, 1994, **13**, 1111; (b) L. G. Hubert-Pfalzgraf, *Polyhedron*, 1994, **13**, 1181.
- 31 (a) R. C. Mehrotra, *Nat. Acad. Sci. Letters*, 1993, **16**, 41; (b) R. C. Mehrotra, *J. Sol-Gel Sci Tech.*, 1994, **2**, 1.